Research Article | Vol. 25, No. 24 | 27 Nov 2017 | OPTICS EXPRESS A1139
Optics EXPRESS

Assessing uncertainties in scattering correction algorithms for reflective tube absorption measurements made with a WET Labs ac-9

NICOLE D. STOCKLEY,[1,*] RÜDIGER RÖTTGERS,[2] DAVID MCKEE,[3] INA LEFERING,[3] JAMES M. SULLIVAN,[1] AND MICHAEL S. TWARDOWSKI[1]

[1]*Harbor Branch Oceanographic Institute, Florida Atlantic University, 5600 US 1 North, Fort Pierce, FL, 34946, USA*
[2]*Helmholtz-Zentrum Geesthacht Centre for Materials and Coastal Research, Max-Planck-Straße 1, 21502 Geesthacht, Germany*
[3]*Physics Department, University of Strathclyde, 107 Rottenrow East, Glasgow, G4 0NG, UK*
**nstockley@fau.edu*

Abstract: In situ absorption measurements collected with a WET Labs ac-9 employing a reflective tube approach were scatter corrected using several possible methods and compared to reference measurements made by a PSICAM to assess performance. Overall, two correction methods performed best for the stations sampled: one using an empirical relationship between the ac-9 and PSICAM to derive the scattering error (ε) in the near-infrared (NIR), and one where ε was independently derived from concurrent measurements of the volume scattering function (VSF). Application of the VSF-based method may be more universally applicable, although difficult to routinely apply because of the lack of commercially available VSF instrumentation. The performance of the empirical approach is encouraging as it relies only on the ac meter measurement and may be readily applied to historical data, although there are inevitably some inherent assumptions about particle composition that hinder universal applicability. For even the best performing methods, residual errors of 20% or more were commonly observed for many water types. For clear ocean waters, a conventional baseline subtraction with the assumption of negligible near-IR absorption performed as well or better than the above methods because propagated uncertainties were lower than observed with the proportional method.

OCIS codes: (010.0280) Remote sensing and sensors; (010.1030) Absorption; (010.4450) Oceanic optics; (280.4788) Optical sensing and sensors.

References and links

1. H. R. Gordon, O. B. Brown, R. H. Evans, J. W. Brown, R. C. Smith, K. S. Baker, and D. K. Clark, "A semianalytic radiance model of ocean color," J. Geophys. Res. Atmos. **93**(D9), 10909–10924 (1988).
2. IOCCG, *Remote Sensing of Inherent Optical Properties: Fundamentals, Tests of Algorithms, and Applications*, Z.-P. Lee ed. (IOCCG, 2006).
3. P. J. Werdell, B. A. Franz, S. W. Bailey, G. C. Feldman, E. Boss, V. E. Brando, M. Dowell, T. Hirata, S. J. Lavender, Z. Lee, H. Loisel, S. Maritorena, F. Mélin, T. S. Moore, T. J. Smyth, D. Antoine, E. Devred, O. H. F. d'Andon, and A. Mangin, "Generalized ocean color inversion model for retrieving marine inherent optical properties," Appl. Opt. **52**(10), 2019–2037 (2013).
4. A. H. Barnard, W. S. Pegau, and J. R. V. Zaneveld, "Global relationships of the inherent optical properties of the oceans," J. Geophys. Res.: Oceans **103**(C11), 24955–24968 (1998).
5. Z. P. Lee, K. L. Carder, R. G. Steward, T. G. Peacock, C. O. Davis, and J. S. Patch, "An empirical algorithm for light absorption by ocean water based on color," J. Geophys. Res.: Oceans **103**(C12), 27967–27978 (1998).
6. D. Stramski, R. A. Reynolds, M. Kahru, and B. G. Mitchell, "Estimation of particulate organic carbon in the ocean from satellite remote sensing," Science **285**(5425), 239–242 (1999).
7. A. Tonizzo, M. S. Twardowski, S. McLean, K. Voss, M. Lewis, and C. Trees, "Closure and uncertainty assessment for ocean color reflectance using measured volume scattering functions and reflective tube absorption coefficients with novel correction for scattering," Appl. Opt. **56**(1), 130–146 (2017).

#307711 https://doi.org/10.1364/OE.25.0A1139
Journal © 2017 Received 22 Sep 2017; revised 31 Oct 2017; accepted 31 Oct 2017; published 10 Nov 2017

Optics EXPRESS

8. J. R. V. Zaneveld, J. C. Kitchen, A. Bricaud, and C. Moore, "Analysis of in situ absorption meter data," Proc. SPIE **1750**, 187–200 (1992).
9. W. S. Pegau, J. S. Cleveland, W. Doss, C. D. Kennedy, R. A. Maffione, J. L. Mueller, R. Stone, C. C. Trees, A. D. Weidemann, W. H. Wells, and J. R. V. Zaneveld, "A comparison of methods for the measurement of the absorption coefficient in natural waters," J. Geophys. Res.: Oceans **100**(C7), 13201–13220 (1995).
10. J. R. V. Zaneveld, J. C. Kitchen, and C. M. Moore, "The scattering error correction of reflecting-tube absorption meters," Proc. SPIE **2258**, 44–55 (1994).
11. R. Röttgers, D. McKee, and S. B. Woźniak, "Evaluation of scatter corrections for ac-9 absorption measurements in coastal waters," Methods Oceanogr. **7**, 21–39 (2013).
12. M. S. Twardowski, J. M. Sullivan, P. L. Donaghay, and J. R. V. Zaneveld, "Microscale quantification of the absorption by dissolved and particulate material in coastal waters with an ac-9," J. Atmos. Ocean. Technol. **16**, 691–707 (1999).
13. J. M. Sullivan, M. S. Twardowski, J. R. V. Zaneveld, C. M. Moore, A. H. Barnard, P. L. Donaghay, and B. Rhoades, "Hyperspectral temperature and salt dependencies of absorption by water and heavy water in the 400-750 nm spectral range," Appl. Opt. **45**(21), 5294–5309 (2006).
14. W. S. Pegau, D. Gray, and J. R. V. Zaneveld, "Absorption and attenuation of visible and near-infrared light in water: dependence on temperature and salinity," Appl. Opt. **36**(24), 6035–6046 (1997).
15. S. Tassan and G. M. Ferrari, "An alternative approach to absorption measurements of aquatic particles retained on filters," Limnol. Oceanogr. **40**(8), 1358–1368 (1995).
16. S. Tassan and G. M. Ferrari, "Measurement of light absorption by aquatic particles retained on filters: determination of the optical pathlength amplification by the 'transmittance-reflectance' method," J. Plankton Res. **20**(9), 1699–1709 (1998).
17. S. Tassan and G. M. Ferrari, "Variability of light absorption by aquatic particles in the near-infrared spectral region," Appl. Opt. **42**(24), 4802–4810 (2003).
18. D. Stramski, S. B. Woźniak, and P. J. Flatau, "Optical properties of Asian mineral dust suspended in seawater," Limnol. Oceanogr. **49**(3), 749–755 (2004).
19. D. Stramski, M. Babin, and S. B. Woźniak, "Variations in the optical properties of terrigenous mineral-rich particulate matter," Limnol. Oceanogr. **52**(6), 2418–2433 (2007).
20. R. Röttgers and S. Gehnke, "Measurement of light absorption by aquatic particles: improvement of the quantitative filter technique by use of an integrating sphere approach," Appl. Opt. **51**(9), 1336–1351 (2012).
21. D. McKee, J. Piskozub, R. Röttgers, and R. A. Reynolds, "Evaluation and improvement of an iterative scattering correction scheme for in situ absorption and attenuation measurements," J. Atmos. Ocean. Technol. **30**, 1527–1541 (2013).
22. R. Röttgers, C. Dupouy, B. B. Taylor, A. Bracher, and S. B. Woźniak, "Mass-specific light absorption coefficients of natural aquatic particles in the near-infrared spectral region," Limnol. Oceanogr. **59**(5), 1449–1460 (2014).
23. E. Leymarie, D. Doxaran, and M. Babin, "Uncertainties associated to measurements of inherent optical properties in natural waters," Appl. Opt. **49**(28), 5415–5436 (2010).
24. M. Jonasz and G. R. Fournier, *Light Scattering by Particles in Water: Theoretical and Experimental Foundations* (Academic, 2007).
25. R. Röttgers, W. Schönfeld, P.-R. Kipp, and R. Doerffer, "Practical test of a point-source integrating cavity absorption meter: the performance of different collector assemblies," Appl. Opt. **44**(26), 5549–5560 (2005).
26. R. Röttgers, C. Häse, and R. Doerffer, "Determination of the particulate absorption of microalgae using a point-source integrating-cavity absorption meter: verification with a photometric technique, improvements for pigment bleaching, and correction for chlorophyll fluorescence," Limnol. Oceanogr. Methods **5**(1), 1–12 (2007).
27. M. S. Twardowski, X. Zhang, S. Vagle, J. M. Sullivan, S. Freeman, H. Czerski, Y. You, L. Bi, and G. Kattawar, "The optical volume scattering function in a surf zone inverted to derive sediment and bubble particle subpopulations," J. Geophys. Res.: Oceans **117**(C7), C00H17 (2012).
28. J. M. Sullivan, M. S. Twardowski, and J. R. V. Zaneveld, "Measuring optical backscattering in water," in *Light Scattering Reviews 7: Radiative Transfer and Optical Properties of Atmosphere and Underlying Surface*, A. A. Kokhanovsky, ed. (Springer-Praxis Books, 2013).
29. W. H. Slade, E. Boss, G. Dall'Olmo, M. R. Langner, J. Loftin, M. J. Behrenfeld, C. Roesler, and T. K. Westberry, "Underway and moored methods for improving accuracy in measurement of spectral particulate absorption and attenuation," J. Atmos. Ocean. Technol. **27**, 1733–1746 (2010).
30. J. Piskozub, Institute of Oceanology of Polish Academy of Sciences, Powstańców Warszawy 55, 81–712 Sopot, Poland (personal communication, 2017).

1. Introduction

Accurate measurements of the inherent optical properties (IOPs) of natural waters are critical to environmental optical research, in particular remote sensing applications. The absorption (a) and backscattering (b_b) coefficients are optical properties closely related to remote sensing reflectance (R_{rs}) [1], forming the link between R_{rs} and the biogeochemical constituents of natural waters. Therefore, they are fundamental parameters in nearly all semi-analytical ocean

color algorithms [2,3], as well as several empirical algorithms [4–6]. Accordingly, the accuracy of these measured IOPs is directly incorporated into the uncertainties in ocean color algorithm development and validation [7].

While progress has been made in developing instrumentation to make in situ measurements of a [8,9], significant sources of uncertainty remain insufficiently characterized. The convention for in situ absorption measurements for the last 25 years has been the multi-spectral (9 wavelengths) ac-9, and its hyperspectral (80 + wavelengths) successor, the ac-s (WET Labs Inc.). These instruments employ a reflective tube approach, relying on an internally reflective flow cell to direct the majority of scattered light towards a diffuse detector. The reflective tube is a quartz cylinder surrounded by an air gap, which theoretically achieves total internal reflectance (TIR) at 41.7°, such that all light scattered at smaller angles would reach the detector and light scattered at larger angles would be excluded [10]. The scattering error (ε) resulting from this excluded light is significant, typically 30-60% of the measured absorption signal at short wavelengths (< 500 nm) and more than 80% at the longer wavelengths (> 650 nm) [11; results herein]. Ideally, ε is given by the integration of the volume scattering function (VSF, β) from the angle (θ) of TIR to π:

$$\varepsilon(\lambda) = 2\pi\int_{\theta_{TIR}}^{\pi} \sin(\theta)\beta(\theta,\lambda)\,d\theta. \quad (1)$$

Equation (1) implicitly includes an angular weighting function for the error, $W(\theta)$, that is 0 below the angle of TIR (all scattered light collected) and 1 above the angle of TIR (all scattered light excluded). Historically, measurements of the VSF have not been available to directly apply such a correction. As a result, several methods [10] have been developed that rely only on the measurements made by the ac meter to correct the measured a for the effects of ε. After first correcting the ac meter data for pure water blanks and pure water temperature and salinity dependencies [12–14], scattering corrected absorption data, $a_{sc}(\lambda)$, is obtained by subtracting the calculated ε from the measured absorption at each wavelength, $a_m(\lambda)$:

$$a_{sc}(\lambda) = a_m(\lambda) - \varepsilon(\lambda). \quad (2)$$

The first and simplest scattering correction method described in Zaneveld et al. [10] defines ε as the measured absorption signal at a near-infrared (NIR) reference wavelength, $a_m(\lambda_{ref})$:

$$\varepsilon(\lambda) = a_m(\lambda_{ref}). \quad (3)$$

This is commonly referred to as the "baseline" or "flat" correction method, conventionally employed in bench top spectroscopy, resulting in a downward shift of the entire absorption spectrum, with $a_{sc}(\lambda_{ref}) = 0$. This method relies on two assumptions: absorption by particulate and dissolved material (a_{pg}) in the NIR spectral region is negligible (i.e., ≤ ~0.002 m^{-1} for a well-calibrated ac-9), so that all of the $a_m(\lambda_{ref})$ signal is due to ε, and that ε is wavelength-independent.

A second [10] method, known as the "constant fraction" method, defines ε as a constant fraction, F, of the measured scattering coefficient, $b_m(\lambda)$, where $b_m(\lambda)$ is the difference between concurrent measurements of attenuation, $c_m(\lambda)$, and $a_m(\lambda)$ from the ac meter, thus:

$$\varepsilon(\lambda) = F\left(c_m(\lambda) - a_m(\lambda)\right). \quad (4)$$

Values of F were estimated [10] to range between about 0.05 and 0.15 for different water types and possible tube reflectivities, although a range of 0.10 to 0.30 appears more likely (see below). This method relies on the assumption that the ratio of ε/b is wavelength-independent. Note this method is complicated by ε also being contained in the b_m term.

Optics EXPRESS

A third [10] method is known as the "proportional" correction and combines the approaches of the first two methods, defining ε spectrally as $a_m(\lambda_{ref})$ weighted by the ratio of $b_m(\lambda)$ and $b_m(\lambda_{ref})$:

$$\varepsilon(\lambda) = a_m(\lambda_{ref})\left(\frac{c_m(\lambda) - a_m(\lambda)}{c_m(\lambda_{ref}) - a_m(\lambda_{ref})}\right). \quad (5)$$

This method relies on assumptions of negligible NIR absorption and a wavelength-independent ε/b ratio. It is becoming increasingly clear that the former assumption may often not apply for many natural environments [11,15–22]. Röttgers et al. [11, their figure 4] in fact determined an empirical relationship between $a_m(715)$ and $a_{pg}(715)$ measured by a point-source integrating cavity meter (PSICAM) with nominally no scattering error from samples collected in the Elbe river estuary and North Sea that can then be used to derive ε:

$$\varepsilon(715) = a_m(715) - 0.212 a_m(715)^{1.135}. \quad (6)$$

If this relationship may be assumed to not vary too much in nature, it may be used to estimate $\varepsilon(715)$, which may then be extrapolated spectrally using either the baseline or proportional methods described above. Or, if an actual measurement of absorption in the NIR, $a_{IC}(\lambda_{ref})$, is available from a device such as PSICAM, which may effectively be considered a reference for "true" absorption, the error may be directly subtracted:

$$\varepsilon(\lambda_{ref}) = a_m(\lambda_{ref}) - a_{IC}(\lambda_{ref}), \quad (7)$$

followed again by some spectral extrapolation method.

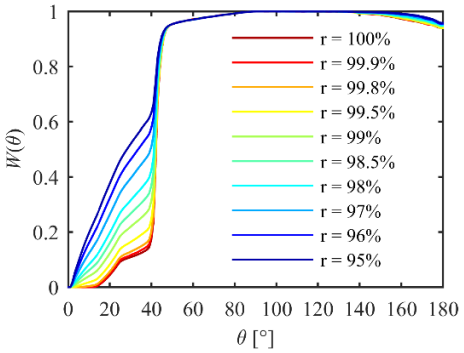

Fig. 1. Weighting functions for absorption flow cell reflectivities (r) from 95% to 100%. (Adapted from [21]).

Recently, McKee et al. [21; also see 23] numerically modeled the weighting function for the scattering error with Monte Carlo simulations. They computed a presumably more accurate weighting function than that implicitly assumed in Eq. (1) for a realistic flow cell, accounting for many possible reflectivities (Fig. 1). Reduced reflectivity may occur either through imperfections in the manufacturing of the tube and/or wear through use. All modeled weighting functions (including the ideal 100% reflectivity case) exhibited non-negligible weightings at angles smaller than the angle of TIR, i.e., the error included significant scattering at these angles. Because β is steeply forward peaked [24], these weighting functions are expected to appreciably increase errors relative to the ideal W implicitly included in Eq. (1). Even small decreases in the reflectivity of the flow tube surface from the ideal value of 100% dramatically increases the amount of scattering in the angular range $0 < \theta < \theta_{TIR}$ from an ideal 0. To explicitly consider W in ε, Eq. (1) becomes:

Optics EXPRESS

$$\varepsilon(\lambda) = 2\pi \int_0^{\pi} \sin(\theta)\beta(\theta,\lambda)W(\theta)\,d\theta. \quad (8)$$

Thus, with a knowledge of $W(\theta)$ through the modeling efforts of [21] and $\beta(\theta)$ from direct concurrent measurements, it may be possible to derive ε independently of the ac device. If $\beta(\theta)$ is known for a limited spectral range, some extrapolation method is also required.

It is important to note that as the number of independently measured variables included in a correction increases, so will propagated errors. Thus, the baseline correction may be expected to have the lowest propagated error, followed by the constant fraction and proportional methods. The method derived from the measured VSF with a spectral extrapolation following the proportional method is expected to have the highest propagated errors of the methods considered herein.

Performance of these corrections is assessed here in data collected from diverse water types during a cruise circumnavigating Great Britain in April 2015. Instrumentation was available to directly determine ε for the application of Eq. (8) for the first time. The Röttgers PSICAM was also employed to provide high quality absorption spectra as the closest estimate of absolute "true" absorption in performance assessments. A key goal of the study was to determine the optimal $W(\theta)$ from Fig. 1 for ac devices using data collected over a broad dynamic range of water types.

2. Methods

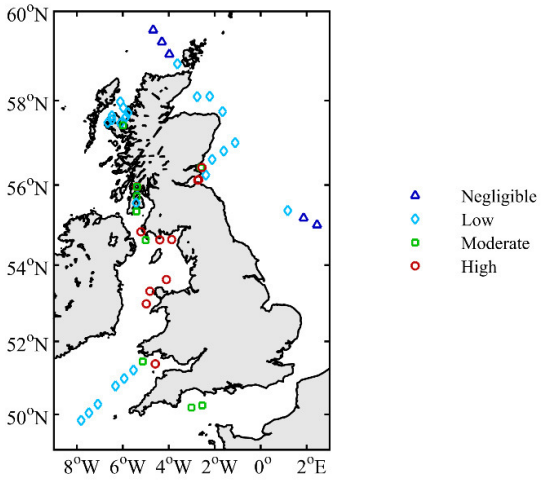

Fig. 2. Map of stations at which IOP data were collected. Colors denote the group based on the magnitude of $a_{pg}(716)$ (see text).

Field data was collected at 62 stations during a cruise conducted in April 2015 aboard the *R/V Heincke* (Fig. 2). At each station, the ship sampling rosette was deployed and water samples were collected at the surface at all stations and occasionally at depth. Spectral absorption was measured in water samples using a PSICAM described in [25,26]. The absorption coefficient of particulate and dissolved material (a_{pg}) of the sample water was measured, using purified water as a reference blank. Corrections for chlorophyll fluorescence and pure water temperature and salinity dependencies were applied, using coefficients specific to the PSICAM [22,26]. The sample water was then filtered using a 0.2 µm membrane filter (GSWP, Millipore) to obtain the absorption coefficient of dissolved material (a_g). In order to account for the difference in spectral bandpasses between the different devices, the PSICAM data (nominally 2 nm resolution) was weighted using a Gaussian function to match the full

Optics EXPRESS

width at half maximum of the ac-9 (FWHM = 10 nm). These FWHM-weighted PSICAM values were then used as the basis for comparison to the measurements made using the WET Labs ac-9.

A separate optical package was also deployed and included a Sea-Bird Electronics 49 FastCAT CTD measuring salinity, temperature, and depth, a WET Labs ac-9 (25 cm pathlength), and a custom Multi-Angle Scattering Optical Tool (MASCOT) [27,28] measuring β from 10° to 170° in 10° increments at a wavelength of 658 nm. Data from these instruments were collected, time stamped, and archived by two WET Labs DH-4 data handlers, with power provided by two battery packs. Data were averaged into 1 m depth bins. The ac-9 was regularly calibrated for drift during the cruise using purified water as a blank and corrections for temperature and salinity dependencies were applied [12]. Since WET Labs ac meters are blanked to pure water, a_{pg} is directly measured. Additionally, measurements of a_g were made using a 0.2 µm membrane capsule filter (Maxi Capsule, Pall) attached to the intake of the ac-9. For comparisons to PSICAM data, three 1 m bins of ac-9 data were averaged together, centered on the recorded depth of the CTD rosette water sample.

MASCOT calibrations and protocols are described in [27]. For application in Eq. (8), the MASCOT β data was extrapolated to the near forward (< 10°) assuming a power law relationship with slope derived from the 10° and 20° measurements, which is typically highly representative for angles < ~70°. While at very small angles β is expected to flatten and thus deviate from the power law, trying to model this effectively is unimportant as there is negligible impact on scattering error in the absorption measurement in this region (see Fig. 1). At angles > 170°, β was assumed equal to $\beta(170°)$. The VSF was then interpolated to 1° resolution using a piecewise cubic hermite interpolating polynomial (pchip function in MATLAB) on a linear scale for the backward direction and on log-log transformed data for the forward direction.

Table 1 summarizes the scattering correction methods for the WET Labs ac-9 as implemented in this work.

Table 1. Summary of scattering correction methods.

Method	Description	Scattering error, ε(λ)
BL	Equation (3)	$a_m\left(\lambda_{ref}\right)$
BL-IC	From Eq. (7), spectrally extrapolated using Eq. (3)	$a_m(715)-a_{IC}(715)$
BL-RR	From Eq. (6), spectrally extrapolated using Eq. (3)	$a_m(715)-0.212a_m(715)^{1.135}$
BL-VSF	From Eq. (8), spectrally extrapolated using Eq. (3)	$2\pi\int_0^\pi \sin(\theta)\beta(\theta,658)W(\theta)d\theta$
FRAC	Equation (4)	$F\left(c_m(\lambda)-a_m(\lambda)\right)$
PROP	Equation (5)	$a_m(715)\left(\frac{c_m(\lambda)-a_m(\lambda)}{c_m(715)-a_m(715)}\right)$
PROP-IC	From Eq. (7), spectrally extrapolated using Eq. (5)	$\left(a_m(715)-a_{IC}(715)\right)\left(\frac{c_m(\lambda)-a_m(\lambda)}{c_m(715)-a_m(715)}\right)$
PROP-RR	From Eq. (6), spectrally extrapolated using Eq. (5)	$\left(a_m(715)-0.212a_m(715)^{1.135}\right)\left(\frac{c_m(\lambda)-a_m(\lambda)}{c_m(715)-a_m(715)}\right)$
PROP-VSF	From Eq. (8), spectrally extrapolated using Eq. (5)	$\left(2\pi\int_0^\pi \sin(\theta)\beta(\theta,658)W(\theta)d\theta\right)\left(\frac{c_m(\lambda)-a_m(\lambda)}{c_m(650)-a_m(650)}\right)$

Optics EXPRESS

3. Results

Over the 62 cruise stations, values for a_{pg} measured by the PSICAM at 412 nm ranged from 0.065 to 0.54 m^{-1}, while $a_g(412)$ ranged from 0.035 to 0.28 m^{-1}. Significant absorption was measured in the NIR spectral region, with the maximum value of $a_{pg}(716)$ near 0.068 m^{-1}. Most of this measurement was due to the particulate fraction, though non-negligible absorption was also measured in the dissolved fraction in most cases, with maximum values of $a_g(716)$ approaching 0.008 m^{-1}.

Of the 62 total stations, complete corrected data sets were available for 54 stations. Several stations were excluded because in situ optical measurements were not made or the instruments had saturated in conditions that exceeded operational limits. In order to consider the performance of each scattering correction method across the range of water types, the 54 stations were arranged in four groups based on the value of $a_{pg}(716)$ measured by the PSICAM (Fig. 3): (1) negligible absorption, $a_{pg}(716) \leq \sim 0.002$ m^{-1} (n = 5); (2) low absorption, $0.002 < a_{pg}(716) < 0.01$ m^{-1} (n = 27); (3) moderate absorption, $0.01 < a_{pg}(716) < 0.03$ m^{-1} (n = 11); and (4) high absorption, $a_{pg}(716) > 0.03$ m^{-1} (n = 11).

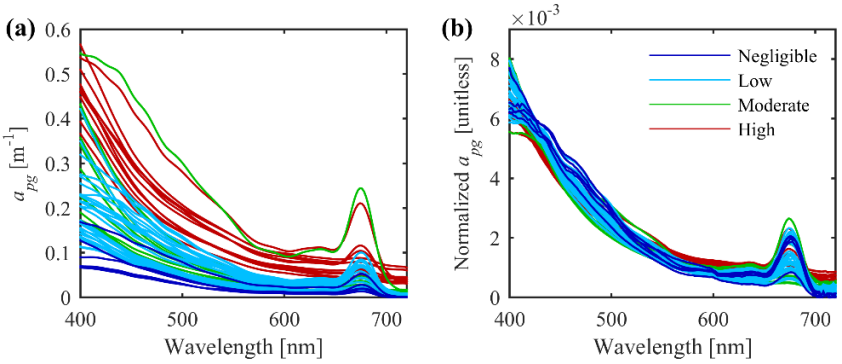

Fig. 3. (a) Absolute a_{pg} spectra measured by the PSICAM at the 54 included stations. Colors denote the group based on the value of $a_{pg}(716)$ described in the text; (b) PSICAM a_{pg} normalized to the spectral integral, $\int_{400}^{720} a_{pg}(\lambda)d\lambda$.

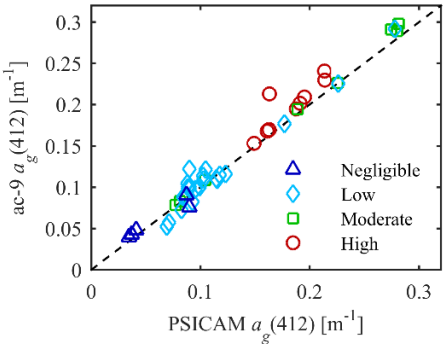

Fig. 4. $a_g(412)$ measured by the ac-9 as a function of FWHM-weighted $a_g(412)$ measured by the PSICAM. The dashed line shows the 1:1 relationship. See text for group descriptions.

To assess overall agreement between the measurement techniques, a_g values measured by the ac-9 were plotted as a function of FWHM-weighted a_g values measured by the PSICAM (Fig. 4). As a result of the exclusion of particles with a 0.2 µm filter, the ac meter a_g values should be unaffected by scattering errors and be nominally equivalent to the PSICAM a_g

values. There was strong agreement between the two instruments, with no significant biases related to magnitude, measurement time, or location.

Results for four selected scattering correction methods are shown for a representative station from each water type group in Fig. 5. Figure 5(a) shows, on an absolute basis, there is little variability among the selected methods and they provide a reasonable match to the PSICAM spectrum for stations where $a_{pg}(715)$ is negligible. In contrast, Fig. 5(d) shows when $a_{pg}(715)$ is high, there is considerably more variation among the methods.

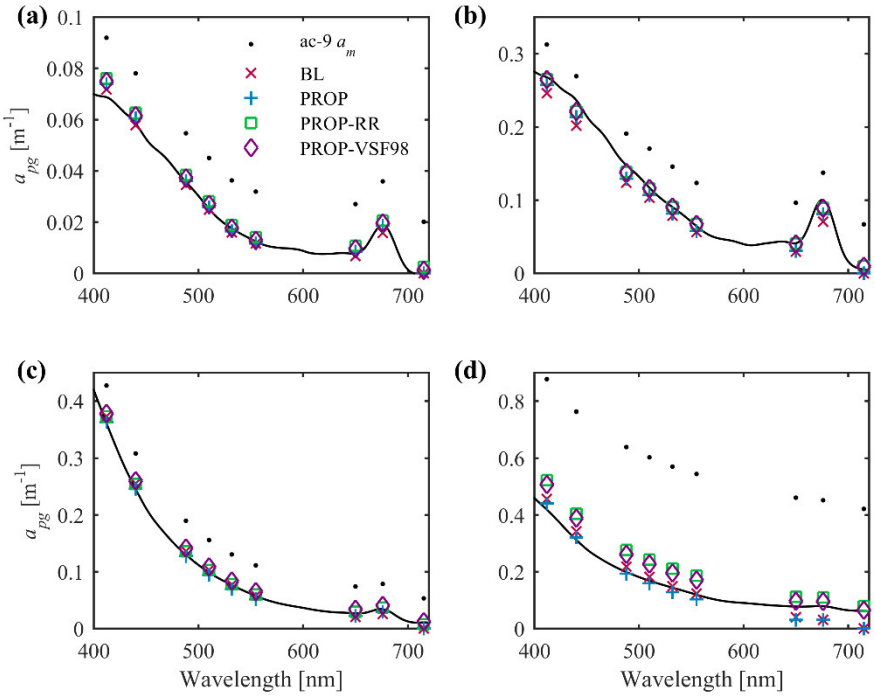

Fig. 5. Representative station from each of the four water type groups: (a) negligible $a_{pg}(716)$; (b) low $a_{pg}(716)$; (c) moderate $a_{pg}(716)$; (d) high $a_{pg}(716)$, showing the spectral fit for selected scattering correction methods. Solid line is the FWHM-weighted PSICAM a_{pg} spectrum.

Each scattering correction method was evaluated both for its performance over the range of observed water conditions and its performance across the absorption spectrum. Performance was assessed using the percent mean error, absolute ($\%\delta_{abs}$) and relative ($\%\delta_{rel}$):

$$\%\delta_{abs} = 100 * \frac{\delta_{abs}}{\bar{y}}, \delta_{abs} = \frac{\sum_{i=1}^{n} |y_i - \hat{y}_i|}{n}; \quad (9)$$

$$\%\delta_{rel} = 100 * \frac{\delta_{rel}}{\bar{y}}, \delta_{rel} = \frac{\sum_{i=1}^{n} (y_i - \hat{y}_i)}{n}; \quad (10)$$

where y is the PSICAM-measured a_{pg} weighted to the FWHM of the ac-9, $\bar{y}$ is the mean of y, and $\hat{y}$ is the ac-9 a_{pg} corrected for ε. The $\%\delta_{rel}$ metric is useful for examining overall biases in the data set, where a value near zero indicates small net bias. The $\%\delta_{abs}$ metric, takes into account the absolute magnitude of the residuals, giving them equal weight, thus representing an aggregate error. Another commonly used metric, percent root mean square error (%RMSE), was not a valid metric for this data set, as match up errors were dominated by bias

Optics EXPRESS

error and thus were not normally distributed. Each wavelength was considered independently from the rest of the spectrum, with n being the number of stations included in each water type group or the entire cruise, as noted.

The BL and PROP methods, the two more commonly used scattering correction methods in the literature, performed similarly to one another, resulting in the best match at short wavelengths (412 – 510 nm) and significantly overestimating ε (underestimating a_{sc}) at long wavelengths (≥ 650 nm) (Fig. 6). Relative agreement between these methods is due to the shared offset subtraction at the reference wavelength (715 nm), as well as similar spectral extrapolations, i.e., the $b_m(\lambda)/b_m(\lambda_{ref})$ proportionality in the PROP method was relatively flat spectrally. Good agreement at short wavelengths between both methods and PSICAM absorption was in part due to the higher magnitudes in this spectral region, but was also due to consistent underestimation in spectral extrapolations that counteracted (serendipitously) the tendency to overestimate due to the inadequacy of the negligible NIR assumption. On both an absolute and relative basis, the BL method showed less variation in the performance of different water types at each wavelength. Compared to the PROP method on a relative basis, the BL method resulted in a lower overestimation of ε at 532 and 555 nm for water types with higher values of $a_{pg}(715)$.

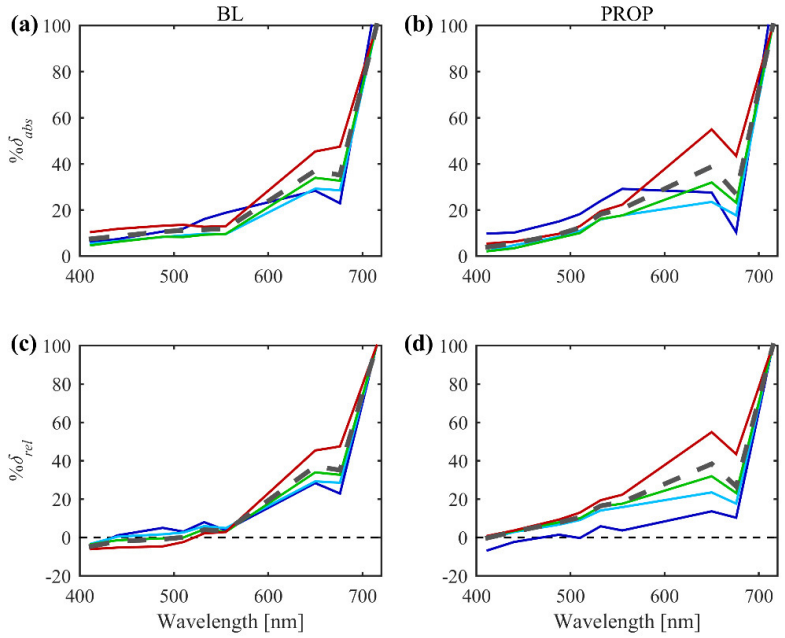

Fig. 6. (a) $\%\delta_{abs}$ for BL method; (b) $\%\delta_{abs}$ for PROP method; (c) $\%\delta_{rel}$ for BL method; $\%\delta_{rel}$ for PROP method. See Fig. 3 for color legend and text for group descriptions. Dashed gray line is for the entire data set (n = 54).

Values of $a_{pg}(716)$ measured by the PSICAM (Fig. 3) provided further evidence that the assumption of negligible absorption in the NIR is not typically valid in natural waters. In order to evaluate the performance of the BL and PROP methods independent of this assumption, the corrected ac-9 $a_{pg}(715)$ was set to the PSICAM-measured (and FWHM-weighted) $a_{pg}(715)$ value. This is referred to here as the "IC' method and was spectrally extrapolated using both of the standard methods. The BL-IC and PROP-IC methods (Fig. 7) performed similarly to one another, again due to the shared offset and similar spectral extrapolations. On an absolute basis, the PROP-IC method outperformed the BL-IC method, except for water with negligible $a_{pg}(715)$, especially for wavelengths between 500 – 650 nm.

Optics EXPRESS

This is due to increasing signal-to-noise ratios at wavelengths with the lowest magnitudes, as propagated errors will always be greater for PROP-based methods. Both BL-IC and PROP-IC resulted in underestimation of ε at shorter wavelengths ($\leq$ 650 nm) for stations with non-negligible $a_{pg}(715)$, the extent of which increased with increasing values of $a_{pg}(715)$. In contrast to the comparison of BL and PROP, on both an absolute and relative basis, the PROP-IC method provided a better match and showed less variability spectrally and across the different water types than the BL-IC method.

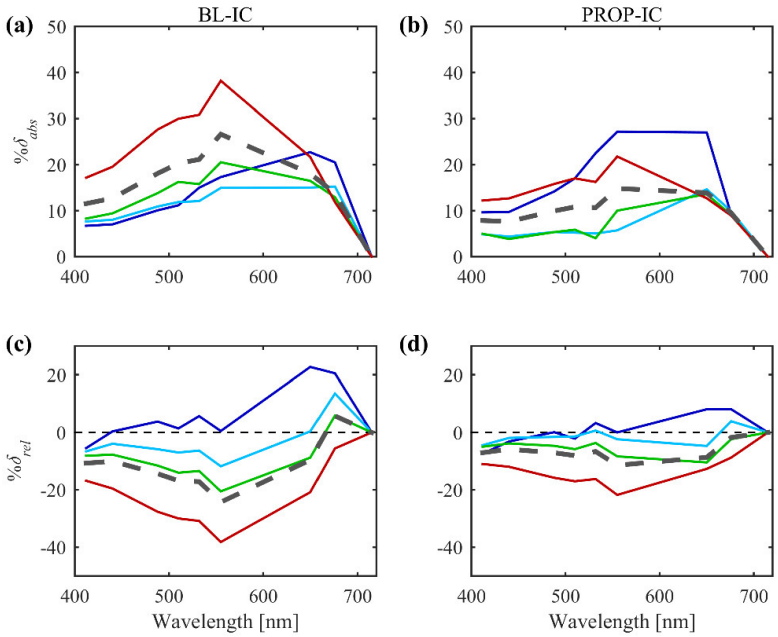

Fig. 7. (a) $\%\delta_{abs}$ for BL-IC method; (b) $\%\delta_{abs}$ for PROP-IC method; (c) $\%\delta_{rel}$ for BL-IC method; $\%\delta_{rel}$ for PROP-IC method. See Fig. 3 for color legend and text for group descriptions. Dashed gray line is for the entire data set (n = 54).

The empirical relationship in Eq. (6), termed the "RR" method, was used to derived $\varepsilon(715)$, which was then spectrally extrapolated with the standard BL and PROP methods. Both the BL-RR and PROP-RR methods again performed similarly to one another, and also to the BL-IC and PROP-IC methods (Fig. 8). Both BL-RR and PROP-RR underestimated ε at most wavelengths (not 676 nm) for all water types (Figs. 8(c) and 8(d)). PROP-IC was generally a better match with less spectral and water type variability. Unlike the comparison of BL-IC and PROP-IC, on an absolute basis, BL-RR and PROP-RR showed greater similarity in the overall fits, with BL-RR performing better for water with negligible $a_{pg}(715)$.

As with the "IC" and "RR" methods, the independent derivation of ε from the VSF (see Table 1) was spectrally extrapolated using the BL and PROP methods. Corrections were assessed using $W(\theta)$ (Fig. 1) representing each flow cell reflectivity modeled in [21]. Closest agreement with the PSICAM (lowest overall absolute error) was obtained for $W(\theta)$ when assuming a reflectivity of 98%. Lower reflectivities produced overestimations of ε at longer wavelengths, with the assumption of 97% reflectivity (BL-VSF97 and PROP-VSF97) giving similar results to the BL and PROP methods. Reflective efficiencies greater than 98% resulted in underestimates of ε at longer wavelengths. BL-VSF98 and PROP-VSF98 (Fig. 9) produced similar results to BL-RR and PROP-RR, with slight underestimations of ε for stations with non-negligible $a_{pg}(715)$.

Optics EXPRESS

A histogram of F from the FRAC method is shown in Fig. 10(a), where the $\%\delta_{abs}$ metric, with $n = 9$ for the ac-9 wavelengths, was used to determine the best value of F for each station when the result was compared to PSICAM a_{pg}. Resulting F values ranged from 10% to over 30%, with the most common being 20%. While using the overall best value of F for a given station provided a good match to the PSICAM data, the range of potential F values makes selection of the most appropriate value difficult without the PSICAM to validate the result. The optimal F for each station at each wavelength was calculated by finding the difference between ac-9 a_m and PSICAM a_{pg} and dividing by b_m at each wavelength. When considered spectrally, this optimal F appeared to decrease slightly with increasing wavelength (Fig. 10(b)). This suggests the assumption of wavelength-independent ε/b may not always be strictly valid, which is consistent with the PROP-IC results from Fig. 7(d). Residual error was observed in PROP-IC after the proportional spectral extrapolation assuming constant ε/b was applied, even though $a_{pg}(715)$ was set equal to the PSICAM value. A strong tendency was observed for higher absorption magnitudes to also have higher F values.

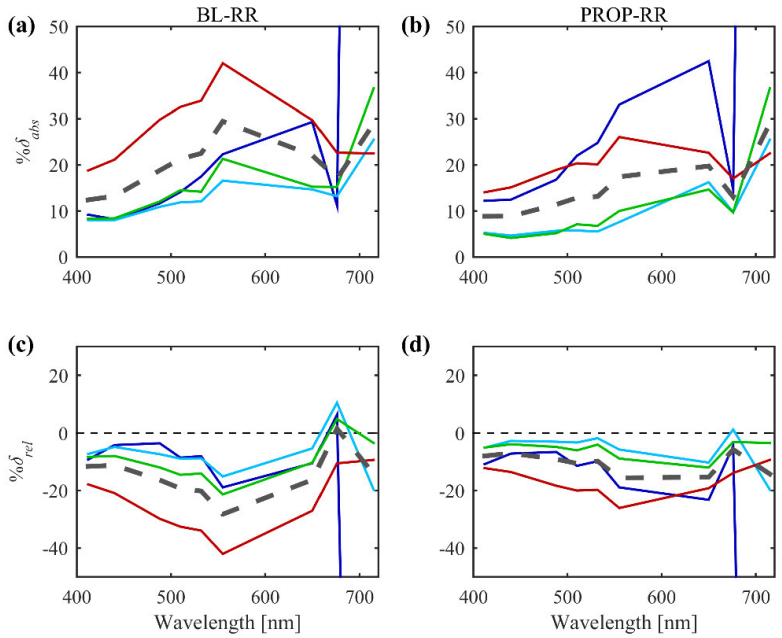

Fig. 8. (a) $\%\delta_{abs}$ for BL-RR method; (b) $\%\delta_{abs}$ for PROP-RR method; (c) $\%\delta_{rel}$ for BL-RR method; $\%\delta_{rel}$ for PROP-RR method. See Fig. 3 for color legend and text for group descriptions. Dashed gray line is for the entire data set ($n = 54$).

4. Discussion

The availability of concurrent measurements of absorption by a WET Labs ac-9 and the PSICAM have allowed for an extensive evaluation of the performance of several reflective tube scattering correction methods. To our knowledge, this is the first time these methods have been evaluated with associated errors in a comprehensive data set covering a wide dynamic range with broad variability in particle composition. This comparison has provided further evidence that one of the assumptions made by the common baseline and proportional methods, that absorption is negligible in the NIR spectral region, is not valid, except for the clearest waters that were sampled. No single correction adequately estimated true absorption at all wavelengths across a wide range of water conditions. Methods experience the greatest difficulty providing accurate estimates in highly absorbing waters and at wavelengths greater than about 600 nm. In fact, residual errors of 20% or more were still observed with the best

performing scattering correction methods. These errors are much higher than in situ measurement errors for other IOPs with state-of-the-art instrumentation [7,28].

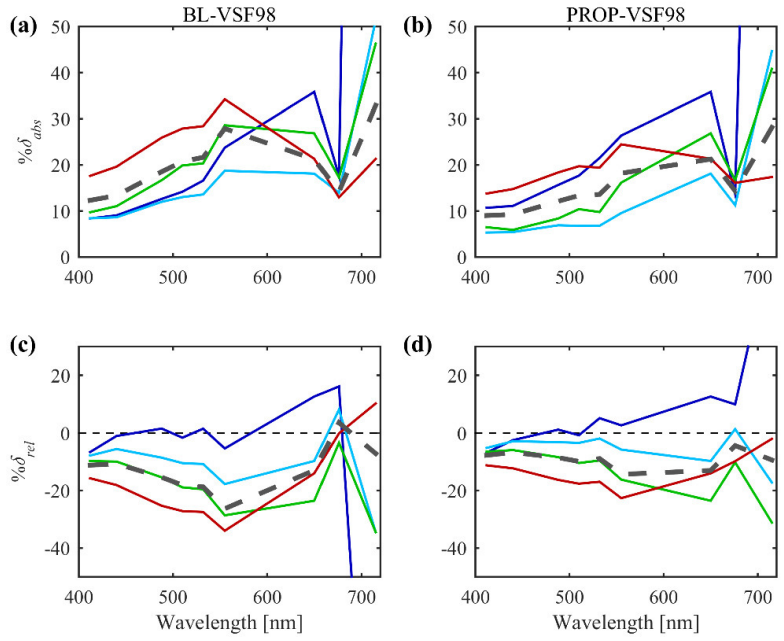

Fig. 9. (a) $\%\delta_{abs}$ for BL-VSF98 method; (b) $\%\delta_{abs}$ for PROP-VSF98 method; (c) $\%\delta_{rel}$ for BL-VSF98 method; $\%\delta_{rel}$ for PROP-VSF98 method. See Fig. 3 for color legend and text for group descriptions. Dashed gray line is for the entire data set (n = 54).

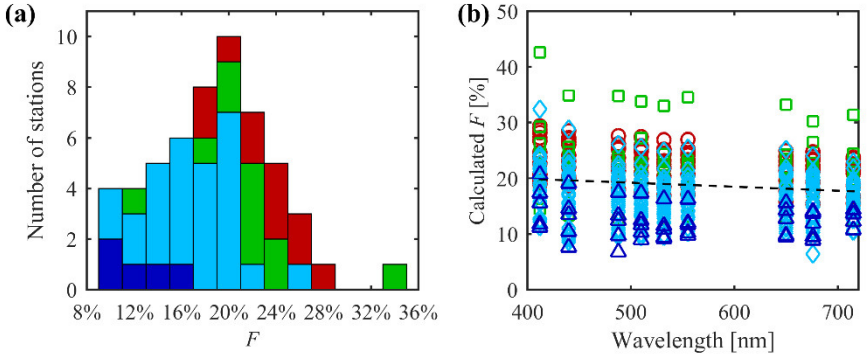

Fig. 10. (a) Histogram of F values for the full spectrum selected from lowest $\%\delta_{abs}$ compared to PSICAM data for the FRAC method; (b) Spectral values of F calculated from the difference between ac-9 a_m and PSICAM a_{pg} at each wavelength for each station. Dotted line is fitted through the mean values from all stations. See Fig. 3 for color legend.

The reference wavelength used for the application of the BL and PROP scattering correction methods was 715 nm, the longest wavelength available for the ac-9. As a_{pg} typically decreases with increasing wavelength > 700 nm, it has been suggested that wavelengths longer than 715 nm may be preferable as a reference for devices such as the WET Labs ac-s [29]. However, $a_{pg}(728)$ was only 2% less on average than $a_{pg}(714)$ in the PSICAM data set, with no significant reduction below the negligible threshold. This result is consistent with the findings in Röttgers et al. [22]. In addition, the temperature dependence of absorption sharply increases in this region, increasing uncertainty without significantly

improving the applicability of the assumption of negligible NIR a_{pg}. Another method that may be employed to improve the applicability of this assumption has been to first subtract a_g from a_{pg}, perform the scattering correction on a_p, and finally add a_g back to the corrected a_p to obtain the corrected a_{pg}. This method removes an a component that is not subject to scattering error. However, a_g is not typically a significant portion of true NIR a_{pg} and problems with the quality of a_g data, including temporal and spatial variability and contamination by bubbles, may further confound application of this method.

Negligible NIR absorption in the BL and PROP corrections was shown to be a poor assumption for many waters, as has been noted previously [11,22]. Furthermore, the results of the IC method showed that even when accounting for non-negligible NIR a_{pg}, neither the BL nor PROP methods provided good fits across the entire spectrum, especially > 500 nm. However, the PROP-IC method had more spectrally consistent errors because low absorption values > 500 nm were more accurate relative to other methods due to a priori knowledge of $a_{pg}(715)$.

The RR method for estimating the NIR scattering error, given by the empirical relationship in Eq. (6), was developed using three data sets collected in Baltic and North Sea coastal waters, with values of $a_{pg}(400)$ measured by the PSICAM ranging from 0.1 to 15 m^{-1} and $a_{pg}(715)$ ranging from ~0.002 to 2.2 m^{-1}. The values of the ac-9 $a_m(715)$ ranged from ~0.01 to nearly 10 m^{-1}. The relationship was determined to be most applicable when $a_m(715)$ > ~0.1 m^{-1}, which corresponds to PSICAM-measured values of $a_{pg}(715)$ > ~0.015 m^{-1}.

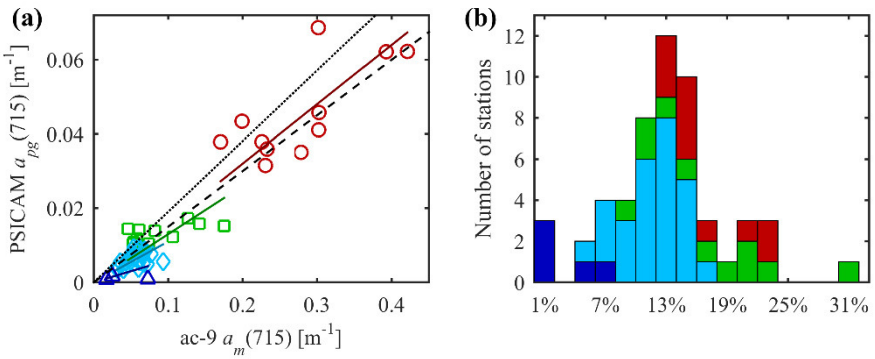

Fig. 11. (a) PSICAM $a_{pg}(715)$ values as a function of ac-9 $a_m(715)$ values. The solid colored lines are the linear fits of each group individually: negligible, 6%; low, 11%; moderate, 13%; high, 16%. The dashed line is a linear fit of all of the data points and the dotted line is the empirical fit from Eq. (6) [11]; (b) Histogram of the percent of ac-9 $a_m(715)$ that is represented by the PSICAM $a_{pg}(715)$.

The relationship between ac-9 $a_m(715)$ and PSICAM $a_{pg}(715)$ was approximately linear for this data set (Fig. 11(a)), with an overall slope for the entire cruise of 15%. Linear fits were forced through zero, consistent with expectation from Beer's Law. Linear slopes were also calculated for each of the four station groups, showing significant increases in the slope with increasing magnitude. The overall cruise slope was primarily driven by the highest magnitude stations. This is further demonstrated in a histogram of the fraction of the ac-9 $a_m(715)$ that was "true," i.e., $a_{pg}(715)$ from PSICAM normalized to the ac-9 $a_m(715)$ (Fig. 11(b)). Results appear consistent with the fit found by Röttgers et al. [11] (a power law relationship deviating slightly from a line), as the values of $a_m(715)$ included in the development of the RR method empirical relationship as noted above extended beyond the highest magnitudes observed here, so a larger effective slope follows the observed trend. At low magnitudes, a wider range in slope values was observed, suggesting a wider range in particle composition and associated particle scattering albedos contributing to the relationship between PSICAM $a_{pg}(715)$ and ac-9 $a_m(715)$. Importantly, uncertainties for the ac-9 were still

better than 10% for nearly all of these samples. At higher magnitudes, this relationship appears to be driven by a more narrow range in particle composition, characterized by stronger relative absorption in the NIR. This observation is consistent with localized re-suspended sediment driving the high magnitude relationships here and in Röttgers et al. [11], and more variable particle compositions driving low magnitude relationships.

For the VSF method, we note that the finding of the best fit using a reflectivity of 98% is supported by two other independent lines of evidence. Errors for multiple reflective flow cells of varying ages were compared using suspensions of barium sulfate ($BaSO_4$), a particle type with broad size distribution and negligible absorption throughout the visible spectrum. The suspension was stabilized with sodium hexametaphosphate to suppress aggregation. Results showed errors for flow cells ranging in age from new to 20 years of heavy use consistently agreed with errors derived from the VSF method with a reflectivity of 98% (Fig. 12). Additionally, Tonizzo et al. [7] obtained the best closure between measured R_{rs} and R_{rs} simulated from IOPs when absorption was corrected using PROP-VSF assuming a reflectivity of 98%. Different flow cells were used in the different studies.

The VSF was only measured at a single wavelength, necessitating the use of the BL and PROP methods for spectral extrapolation. The results found here may improve if spectral VSF data was available, and if measurements included the near forward (< 10°) to avoid uncertainty associated with angular extrapolation. While weightings for the scattering error are low in this angular region (Fig. 1), the magnitude of the VSF increases dramatically, so the net contribution is significant, between 10 and 40% of the total scattering error for the 98% reflectivity $W(\theta)$. Improvements in the modeling of the weighting functions from [21] may also be possible [30]. What can be stated definitively at this time is the specific VSF extrapolation method used here, coupled with the modeled weighting function from [21] with 98% reflectivity, consistently provided the closest match to our best estimate of true absorption from the PSICAM. Further application of the method in this manner would be expected to carry similar errors to those determined here.

While the VSF method performed similarly to the RR method for this data set, one may expect the VSF method to be more universally applicable to a wide range of water conditions, as ε is directly derived. However, the requirement of independent measurement of the VSF is obviously an obstacle in implementation, as there are few devices available to make these measurements.

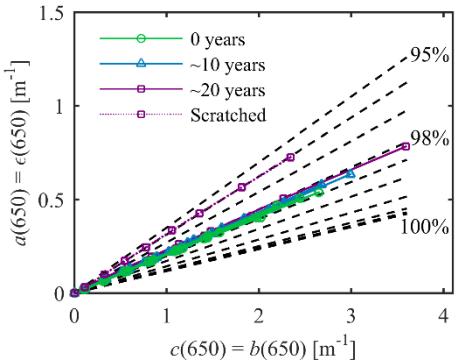

Fig. 12. Results of a $BaSO_4$ suspension series showing the variability of ε for 5 different ac reflective flow cells of approximately three different ages. One of the tubes was then reassessed after the inside was scoured with steel wool and sandpaper (not recommended in practice) in an effort to intentionally modify the reflectivity. Dashed lines are errors derived from Eq. (8) using MASCOT phase function measurements and the weighting functions for different reflectivities shown in Fig. 1 from [21].

Optics EXPRESS

5. Conclusions

Spectral absorption measurements using a WET Labs ac-9 meter were collected, scattering corrected using several methods, and compared to measurements made by a PSICAM to assess performance over a wide range of water conditions. Overall, correction methods PROP-RR and PROP-VSF98 performed best, as determined with the absolute error metric. While similar, the favorable performance of PROP-RR is encouraging as it does not rely on independent VSF measurements. As such, it may be readily applied to historical data.

There are several caveats in the above conclusions, however. In the clearest waters, BL-RR performed better than PROP-RR because of enhanced error propagation with the PROP-RR method. There was also a larger range in slopes between PSICAM $a_{pg}(715)$ and ac-9 $a_m(715)$ for ac-9 $a_m(715)$ magnitudes < 0.1 m^{-1}, a subset that includes most coastal ocean and virtually all open ocean waters (Fig. 11). Thus, while BL-RR or simply BL may be the most appropriate correction method for very clear waters, ambiguity remains about the application of PROP-RR in the important "low" magnitude absorption range. For high magnitudes, the effects of re-suspended clay-dominated sediments are presumably well documented here and in [11], but for waters where other types of non-algal absorbing particles may be present in higher proportions, it is unclear whether the PROP-RR relationship will remain appropriate. Considering these caveats, the independent PROP-VSF98 method with directly derived correction may have more widespread applicability.

For the constant fraction method, the range of F values observed makes a priori selection of the most appropriate value difficult without ancillary data on particle composition and concentration. If the optimal F value could be linked to another commonly measured parameter (e.g., b_b/c; see [21]), some adaptation of the method may prove viable as a scattering correction. This is an area of ongoing work.

Perhaps the most important conclusion is none of the considered scattering correction methods resulted in ac-9 absorption spectra that accurately matched the shape and magnitude of the PSICAM measurements across the range of water types. As such, further efforts are needed in developing improved corrections, as well as developing new technologies for determining in situ absorption that are less influenced by such errors.

Funding

National Aeronautics and Space Administration (NASA) (NNX15AN17G); Alfred Wegener Institute (AWI_HE442_00); Harbor Branch Oceanographic Institute Foundation.

Acknowledgments

The authors would like to thank the crew of the *R/V Heincke* for their assistance and dedication during the cruise. Discussions with Alberto Tonizzo aided analysis. Comments from Jacek Piskozub and an anonymous reviewer improved an earlier version of the manuscript.